AD-A080 316 TEXAS UNIV AT AUSTIN DEPT OF CHEMISTRY F/G 9/1
SEMICONDUCTOR ELECTRODES. 24. BEHAVIOR AND PHOTOELECTROCHEMICAL--ETC(U)
DEC 79 F F FAN, A J BARD N00014-78-C-0592
UNCLASSIFIED NL

1 OF 1
AD A080316

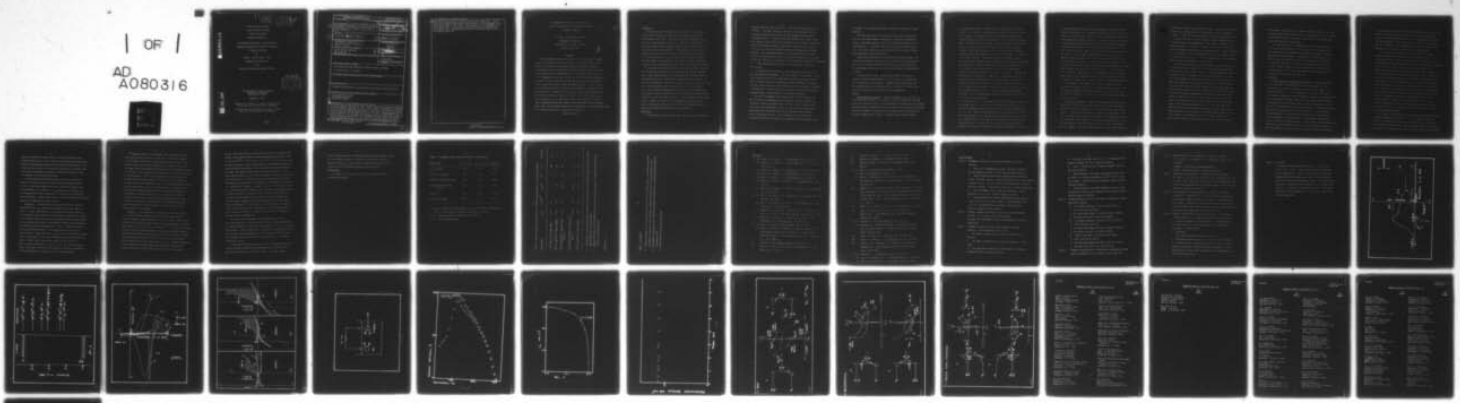

END
DATE FILMED
3-80
DDC

OFFICE OF NAVAL RESEARCH

Contract N00014-78-C-0592

Task No. NR 051-693

TECHNICAL REPORT No. 5

Semiconductor Electrodes. 24. Behavior and Photoelectrochemical Cells Based on p-Type GaAs in Aqueous Solutions

by

Fu-Ren F. Fan and Allen J. Bard

Prepared for Publication

in the

Journal of the American Chemical Society

The University of Texas at Austin
Department of Chemistry
Austin, Texas 78712

December 1, 1979

SECURITY CLASSIFICATION OF THIS PAGE (When Data Entered)

REPORT DOCUMENTATION PAGE

READ INSTRUCTIONS BEFORE COMPLETING FORM

1. REPORT NUMBER: 5

2. GOVT ACCESSION NO.

3. RECIPIENT'S CATALOG NUMBER: Technical rept. no. 5

4. TITLE (and Subtitle): Semiconductor Electrodes. 24. Behavior and Photoelectrochemical Cells Based on p-Type GaAs in Aqueous Solutions.

5. TYPE OF REPORT & PERIOD COVERED: 1 Sept [redacted] 79 to 31 Aug [redacted] 80

6. PERFORMING ORG. REPORT NUMBER

7. AUTHOR(s): Fu-Ren F. Fan [redacted] Allen J. Bard

8. CONTRACT OR GRANT NUMBER(s): N00014-78-C-0592

9. PERFORMING ORGANIZATION NAME AND ADDRESS
Department of Chemistry
University of Texas at Austin
Austin, TX 78712

10. PROGRAM ELEMENT, PROJECT, TASK AREA & WORK UNIT NUMBERS: 12 41

11. CONTROLLING OFFICE NAME AND ADDRESS
Office of Naval Research
800 N. Quincy
Arlington, VA 22217

12. REPORT DATE: 1 Dec [redacted] 1979

13. NUMBER OF PAGES: 36

14. MONITORING AGENCY NAME & ADDRESS (if different from Controlling Office)

15. SECURITY CLASS. (of this report): Unclassified

15a. DECLASSIFICATION/DOWNGRADING SCHEDULE

16. DISTRIBUTION STATEMENT (of this Report)

This document has been approved for public release and sale;

its distribution is unlimited.

17. DISTRIBUTION STATEMENT (of the abstract entered in Block 20, if different from Report)

18. SUPPLEMENTARY NOTES

Prepared for publication in the Journal of the American Chemical Society.

19. KEY WORDS (Continue on reverse side if necessary and identify by block number)

semiconductor electrodes
photoelectrochemistry
Fermi level pinning

20. ABSTRACT (Continue on reverse side if necessary and identify by block number)

The electrochemical Behavior of single crystal p-type GaAs in aqueous solutions containing several redox couples (I_3^-/I^-, Fe(III)/Fe(II), Sn(IV)/Sn(II), Eu(III)/Eu(II)) in the dark and under irradiation is described. The observation that the difference in potential between that for the onset of photocurrent and the standard potential for the redox couple was 0.4 to 0.5 V, independent of the couple, leads to a revised model for semiconductor/electrolyte solution interface with semiconductors having a high density of surface states with energies within the band gap region. In such a surface controlled system, the Fermi

DD FORM 1 JAN 73 1473 EDITION OF 1 NOV 68 IS OBSOLETE
S/N 0102-014-6601

Unclassified 347 830
SECURITY CLASSIFICATION OF THIS PAGE (When Data Entered)

level of the semiconductor is pinned at the surface state level. Several solar cells in which p-GaAs shows stable behavior are described. The cell p-GaAs/I_3^- (0.25 M), I^- (0.75 M)/Pt showed an open circuit voltage of 0.20 V and a short circuit current density of 30 mA/cm^2 under irradiation with 1.7 mW He-Ne laser. The quantum efficiency at the maximum photocurrent in this cell was about 95%.

Semiconductor Electrodes. 24. Behavior and Photoelectrochemical Cells Based on p-Type GaAs in Aqueous Solutions

Fu-Ren F. Fan and Allen J. Bard
Department of Chemistry
The University of Texas at Austin
Austin, Texas 78712

(ABSTRACT)

The electrochemical behavior of single crystal p-type GaAs in aqueous solutions containing several redox couples (I_3^-/I^-, Fe(III)/Fe(II), Sn(IV)/Sn(II), Eu(III)/Eu(II)) in the dark and under irradiation is described. The observation that the difference in potential between that for the onset of photocurrent and the standard potential for the redox couple was 0.4 to 0.5 V, independent of the couple, leads to a revised model for semiconductor/electrolyte solution interface with semiconductors having a high density of surface states with energies within the band gap region. In such a surface controlled system the Fermi level of the semiconductor is pinned at the surface state level. Several solar cells in which p-GaAs shows stable behavior are described. The cell p-GaAs/I_3^- (0.25 M), I^- (0.75 M)/Pt showed an open circuit voltage of 0.20 V and a short circuit current density of 30 mA/cm^2 under irradiation with the full visible (longer than 590 nm and IR filtered) output from a 450 W Xe-lamp focused onto the photocathode. The quantum efficiency at the maximum photocurrent in this cell was about 95%.

(End of Abstract)

Introduction

Considerable success has been realized recently[1-3] in converting visible light to electricity using n-type semiconductor-based photoelectrochemical (PEC) cells. In principle, p-type semiconductors should be useful as photocathodes in a PEC cell. Some p-type semiconductor electrodes studied to date, p-MoS_2, p-CdTe, p-GaAs or p-GaP, seem to be stable when used as photocathodes[4-8]. Unfortunately, the onset photopotential for the PEC reaction on most p-type electrodes lies negative of the flat-band potential, V_{fb}, and close to the standard potential of the redox couple in the electrolyte. This limits the open circuit photovoltage of p-type semiconductor-based PEC cells to relatively small values.

In this paper we describe PEC effects on p-GaAs electrodes. We show that the quantum efficiencies of these PEC cells are strongly dependent on the redox couples present in the solution and the "one-third rule" in semiconductor physics[9] is applicable to explain the present results. In addition, we demonstrate a p-GaAs based solar cell in an I^-/I_3^- system. The short-circuit quantum yields for electron flow of this cell approach 100%. Under short-term illumination with the full visible (longer than 590 nm and IR filtered) output from a 450 W Xe-lamp focused onto the photocathode, the p-GaAs electrode was stable. To our knowledge this represents the first example of a single p-type semiconductor-based PEC cell in aqueous solution which shows near 100% short-circuit quantum efficiency under fairly strong light intensity with good stability.

Experimental

The semiconductors used are p-type GaAs single crystals obtained from

Atomergic Chemicals (Long Island, N.Y.). The acceptor concentration was $3x10^{18} cm^{-3}$. The ohmic contact was obtained by electroplating Au on the rear surface (which was polished first with sandpaper and then with 0.5 μm alumina on felt). A copper wire was then attached to the ohmic contact with conductive silver epoxy (Allied Products Corp., New Haven, Connecticut) which was subsequently covered, along with the copper wire and the sides of the crystal, with silicone rubber sealant (Dow Corning Corp., Midland, Michigan). The semiconductor material was then mounted onto an 8" long piece of 7 mm diameter glass tubing, resulting in an exposed area of p-GaAs of 0.05 cm^2. Before use, the surface of the electrode was etched for 10-15 seconds in concentrated H_2SO_4:30% H_2O_2:H_2O (3:1:1) followed by 6 M HCl for 10-15 seconds.

A conventional three-electrode, single-compartment cell was used for the electrochemical measurements. The electrochemical cell (volume ≅ 25 ml.) which contained the Pt disk or semiconductor working electrode was fitted with a flat Pyrex window for illumination of the semiconductor. Removable air-tight Teflon joints were used with the Pt disk or semiconductor electrode. A platinum foil (~40 cm^2) was used as the counter electrode and an aqueous saturated calomel electrode (SCE) as the reference electrode.

The cyclic voltammograms were obtained with a PAR 173 Potentiostat, PAR 175 Universal Programmer and PAR 179 Current-to-Voltage Converter and recorded on a Houston Instruments Model 2000 X-Y recorder (Austin, Texas). In the solar cell measurements, current (i) and voltage (V) readings were taken between the working electrode and the platinum counter electrode with no external power source. The photovoltage and the photocurrent as functions of the load resistance were measured with a Keithley Model 600A

electrometer or a custom-built voltage follower and a current-to-voltage converter.

The light source used in the study of the PEC effect was an Oriel Corp. 450 W Xe-lamp (Stamford, Connecticut). Experiments designed for specific wavelengths employed an Oriel 7240 grating monochromator with a 20 nm band pass. A red filter (590 nm cut-on) was used with the xenon lamp. The radiant intensity was measured with an EG & G Model 550 Radiometer/Photometer (Salem, Massachusetts).

Reagent grade chemicals were used without further purification. All solutions were prepared from triply distilled water and were deoxygenated for at least 30 minutes with purified nitrogen before each experiment. All experiments were carried out with the solution under nitrogen without stirring.

A Perkin-Elmer 303 atomic absorption spectrometer fitted with a standard Ga hollow cathode operated at 2874 Å was used to determine the Ga^{3+} concentration in the solution. Standard solutions containing Ga^{3+} were prepared from a stock solution of $GaCl_3$ (200 ppm Ga^{3+}) with the same electrolyte solution as used in the solar cell measurement.

Results

Current-potential behavior. - Typical voltammetric curves in the I^-/I_3^- system are shown in Figure 1. As shown in curve 1, the dark anodic current, which starts at about 0.28 V vs. SCE, represents the oxidation of iodide through the valence band of p-GaAs;[6] this reaction competes with the anodic dissolution. The rate of oxidation of iodide on p-GaAs is much smaller than that at a Pt electrode (compare curves 1 and 3). Negligibly small cathodic currents

were observed for p-GaAs in the dark (curve 1), as expected for a p-type material (i.e., with only a small density of minority carriers, electrons, at the surface). The cathodic current was substantially enhanced under illumination, because electrons are promoted by the light into the conduction band. An implication of these results is that the reduction rate of iodine on p-GaAs is limited by the electron density at the surface of p-GaAs electrodes rather than the energetic factor. Under constant illumination a cathodic photocurrent commencing at ~0.75 V vs. SCE (curve 2) is observed at the p-GaAs electrode. The photocurrent during a potential sweep in unstirred solution reached a maximum at about 0.32 V vs. SCE before decreasing. The decrease in the cathodic photocurrent at potentials negative of 0.32 V is attributed to mass transfer effects, since it can be eliminated by vigorous stirring of the solution (see curves 2-a and 2-b). Note that the photocurrent for triiodide (I_3^-) reduction lies at potentials positive of the potentials for the reduction of I_3^- on Pt electrodes; this potential difference represents the conversion of light to electrical energy. From the i-V curves on Pt and p-GaAs one predicts that a PEC cell based on p-GaAs and platinum electrodes in an I^-/I_3^- solution should show high quantum efficiency. This is indeed observed and will be illustrated by the results of the solar cell described below.

In the absence of I_3^-, the cathodic photocurrent decreases to negligibly small values (curve 4). Even in this acidic medium in the absence of I_3^-, significant hydrogen evolution was only observed at potentials negative of -0.2 V vs. SCE. Clearly, the photoreduction of I_3^- competes very well with the hydrogen formation; from the band structure predicted from V_{fb} of p-GaAs in this medium[10] (Fig. 2), H^+ reduction is energetically possible by photogenerated electrons. The lack of reduction of H^+ under these conditions suggests that the GaAs does not have the properties characteristic of "low

hydrogen overpotential" surfaces. The photoreduction of several other couples at p-GaAs were also investigated (Table 1); with all of the redox couples, all oxidized forms, except for Fe(III), compete well with protons for photogenerated electrons on p-GaAs. As shown in Figure 3, even heptyl viologen^{+}/heptyl viologen^{2+} and Eu(II)/Eu(III), which have more negative standard redox potential (-0.43 V vs. NHE) than that of H_2/H^+ (0.0 V vs. NHE at pH 0) are able to compete fairly well with the hydrogen evolution. The ring (Pt) - disc (p-GaAs) electrode experiment on Eu(II)/Eu(III) by Memming[10] showed that almost 100% of the cathodic photocurrent is due to the photoreduction of Eu(III). In the case of heptyl viologen, a film of insoluble, violet, heptyl viologen^{+} bromide could be deposited on the p-GaAs under illumination by applying a potential about -0.25 V vs. SCE on the p-GaAs electrode. Applications of the p-GaAs/HV^{2+} Br^- system to electrochromic devices and rechargeable solar cells will be discussed elsewhere. The behavior of several other systems at p-GaAs is illustrated in Figure 4.

The voltammetric data summarized in Table 1 show that the onset potentials for the PEC reactions vs. the standard potentials, V_{on}-V°, are only slightly dependent on the redox couples used in this study. V_{on}-V° for Eu^{2+}/Eu^{3+} is about 0.50 V, which is close to one-third of the band gap of GaAs (E_g=1.4 eV).

Solar cell measurements. - Regenerative semiconductor/liquid junction photovoltaic (solar) cells are fabricated by immersing the semiconductor electrode and a counter electrode in a solution containing a redox couple (Figure 5). With n-type semiconductors, which act as photoanodes in the cells, the redox couple often serves to stabilize the semiconductor against photo-oxidation. While a number of cells with n-type materials (e.g. GaAs, CdS, CdSe) have been described, stable cells with p-type semiconductors are less frequent. Solar cells were formed with a p-GaAs photocathode and

a platinum foil anode with various redox couples. The open-circuit photovoltages (V_{oc}) and the short-circuit photocurrents (i_{ss}) are summarized in Table II. Eu^{2+}/Eu^{3+} showed the highest open-circuit photovoltage while I^-/I_3^- produced the largest i_{ss} and showed the highest quantum efficiency. As shown in Figure 6, at monochromatic light intensity 5-8 mW/cm^2, the quantum efficiency of a p-GaAs/I^-(0.75M), I_3^-(0.25 M), H^+(1.0 M)/Pt PEC cell at wavelengths shorter than 750 nm approaches 100%, if light absorption by I_3^- is minimized. The i-V characteristic of this cell, shown in Figure 7, yields a fill factor of 0.65. This cell showed highly stable operation, with no evidence of decomposition of the p-GaAs.

Irradiation of the p-GaAs crystal with the full visible (longer than 590 nm and IR filtered) output from a 450 W xenon lamp focused onto the photoelectrode surface yielded a stable ~23 mA/cm^2 photocurrent (Figure 8). No attempt was made to minimize the optical absorption due to I_3^- (the optical path through the solution was about 1 cm). The power efficiency under these conditions was estimated to be about 5-6%. If the solution was stirred and/or the optical path through the solution was minimized, the photocurrent could be increased to higher levels (~35 mA/cm^2). During a seven-hour continuous illumination, the stability of the p-GaAs photocathode was demonstrated by (1) a constant photocurrent, (2) no obvious change in the appearance of the electrode surface, and (3) no detectable amount of Ga^{3+} produced by decomposition (i.e., less than 1 ppm, the detection limit of the flame atomic absorption spectrometer used in this study, was detected in the solution after the experiment) (Table II). This result indicates that photodecomposition of the GaAs, assumed to be a three-electron reaction, can represent no more than ~0.02% of the total

photocurrent. The possibility of chemical attack of GaAs by I_3^- was also checked by keeping the p-GaAs electrode in contact with the I^-/I_3^- solution in the dark for one day. Less than 1 ppm of Ga^{3+} was determined by the flame atomic absorption spectroscopy.

As shown in Table II, the quantum efficiencies of p-GaAs based PEC cells are strongly dependent on the redox couples. The quantum yields for electron flow can be substantially enhanced by applying a negative potential on the photocathode. For example, for irradiation with a 1.6 mW He-Ne laser (632.8 nm) of a p-GaAs photocathode in Sn^{2+} (0.5 M)/Sn^{4+} (0.5 M) (1 M H^+ and 6 M Br^-), the short-circuit quantum efficiency was only 16%. However by applying a negative potential to the GaAs to bring its potential to -0.5 V vs. SCE, the quantum yield for electron flow was increased to about 86% (see Table II).

Discussion

Surface barrier at p-GaAs/solution interface. - The results given in Table I show that the difference between the onset potential for the photocurrent, V_{on}, and the standard potential of the redox couple, V°, ΔV, is generally about 0.4 - 0.5 V, independent of V° for the redox couple. These results, coupled with previous findings for p-GaAs in acetonitrile[1d, 1e] and liquid ammonia[11] solutions, suggest that the simple idealized model for a semiconductor/solution interface must be modified to account for the behavior.[12] The ideal model for the interface (Figure 9a)[13] would predict that V_{on} would be near V_{fb} and that ΔV would vary with V°. Previous studies have shown, however, that dark oxidations can occur at p-type materials (or dark reduction at n-type materials), even for couples with energies located within the forbidden gap region. These dark reactions at potentials, where there is not appreciable overlap of the redox solution distribution with the conduction or valence band carrier densities, have been attributed

to charge transfers via surface states or intermediate levels in the gap region. They also constitute a path for loss of the photogenerated species by surface recombination, e.g., for p-type materials the photogenerated reductant, R, can be oxidized via such levels as suggested in Fig. 9b. The effect of this recombination is a smaller ΔV with a lower dependence on V° than that predicted from the idealized model.

If the surface state density is high, the nature of the semiconductor/solution interface might best be described as surface layer controlled (Fig. 9c). This is analogous to the effect found at a metal/semiconductor Schottky barrier when the density of surface states is high.[9a] In this case these states absorb most of the charge transferred to equalize the Fermi levels, thus "pinning" the Fermi level of the metal at this energy independent of the metal work function. What is observed in this case is a constant barrier height between bulk semiconductor (e.g. GaAs) and metal. For the solution case this is equivalent to "pinning" of the semiconductor Fermi level at the redox potential of the solution couple with all of the photovoltage developed between the semiconductor surface and bulk (Fig 9c). Such a surface controlled model, modified for effects of recombination, appears to be appropriate for the p-GaAs/solution interface. Moreover the ΔV value found, ~0.4 - 0.5 V, is consistent with surface states located at a position predicted by the "one-third rule"[9], i.e., at energies one-third of E_g (1.4 eV for GaAs) up from the valence band edge.

This surface controlled model is also consistent with previous studies of GaAs in nonaqueous solvents.[1d, 1e, 11] For example in studies of acetonitrile solutions it was necessary to invoke surface layers on the GaAs to explain photoeffects for couples located well above the conduction band edge. This proposed surface layer can be considered to be the surface

modified by filling the surface states, in this case moving the semiconductor Fermi level up to the location of the solution redox couple while maintaining band bending between the surface and bulk semiconductor. Such a model can also account for the observed photoejection of electrons from p-GaAs into liquid ammonia at potentials considerably negative of those corresponding to the conduction band edge.

The semiconductors which should exhibit this surface controlled behavior are those which exhibit similar behavior with metal Schottky barriers. Such studies suggest that surface controlled behavior occurs in semiconductors of low ionicity, as represented by the difference in electronegativities of the constituents.[14] Thus GaAs, Si, and InP would show such behavior. Indeed recent studies of InP in acetonitrile[15] and p-Si[16] suggested the importance of surface effects.

Solar cells. - The open circuit photovoltage of the two electrode photovoltaic cells, V_{oc}, should ideally approach the ΔV-value given in Table I. In most cases however V_{oc} was significantly smaller (Table II). This difference can be ascribed to the dark anodic current which is present in the potential region for the onset of the photocurrent with most couples. The V_{on} represents the onset of the modulated or phase sensitive-detected photocurrent which occurs superimposed on a net d.c. dark anodic current. The V_{oc}-value represents the d.c. photovoltage which will be at less positive values. Significantly the V_{oc} value for the Eu(III)/Eu(II) system, which is well negative of the anodic decomposition current of the GaAs, is largest. Similar effects have recently been seen for p-GaAs in a methyl viologen electrolyte (V°= -0.66 V vs. SCE). For the Sn(IV)/Sn(II) couple, the system is slow even at Pt (Figure 4c) and this too contributes to the low operating cell voltage even at very small currents.

The quantum efficiency is determined by the spectrum of the light source and the spectral response of the cell. The spectral response in turn depends on the optical absorption coefficient, the width of the depletion region, the lifetime and mobilities of charge carriers, and the charge transfer and recombination kinetics at the semiconductor/electrolyte interface. All parameters except the last one are mainly controlled by the semiconductor. The different quantum efficiencies observed for the different redox couples (Table II) will thus be due to differences in charge transfer and recombination rates. The limiting quantum efficiency for every redox couple occurs at a potential about 0.3 V negative of the redox potential, suggesting that the extent of band-bending within the semiconductor is about the same for each, as expected for a surface controlled system. Hence, the different limiting quantum yields shown in Table II are not due to different widths of the depletion layer but mainly contributed by different charge transfer kinetics at the semiconductor/electrolyte interface.

Stability. - From thermodynamic considerations alone, GaAs (either p- or n-type) should be stable only over a very restricted range of potentials and pH in aqueous solutions.[17c] In fact, however, n-GaAs can be stabilized with respect to photo-oxidation by the incorporation of suitable redox couples (e.g. Se_2^{2-}/Se^{2-}) in the solution.[2b, 3b] This has been explained in terms of the redox couple maintaining a surface potential more negative than that for the anodic dissolution reaction.[17a,b] With respect to p-GaAs stabilization requires that no oxidation of the GaAs occurs by reaction with the oxidized form of the redox couple (e.g., I_3^-). Indeed illumination of the p-GaAs tends to cathodically protect the material from such an oxidative corrosion reaction by generating electrons at the electrode

surface. The materials must also be stable with respect to cathodic decomposition, which requires that the cathodic decomposition potential (-0.8 V vs. NHE at pH 0[10]) of the p-GaAs be more negative than the location of the conduction band edge or that a redox couple is present which can maintain a surface potential more positive than the cathodic decomposition potential of p-GaAs. The present results show that the redox process of I^-/I_3^- at p-GaAs photoelectrodes can occur during illumination without any significant anodic dissolution. The question arises, then, which factors other than thermodynamic considerations are of importance in determining the stability of a semiconductor electrode. It appears in this case that kinetic factors and surface states play an important role. We suggest that chemical attack or anodic dissolution is kinetically very slow and the photo-protection from these reactions might be very efficient, if the quasi-Fermi level for holes under illumination does not substantially deviate from that at thermal equilibrium.[17a] In this respect, a p-type material, especially a surface state controlled p-type semiconductor, has the advantage that its quasi-Fermi level for holes is relatively insensitive to the change of hole density due to illumination.

The results above show that p-type semiconductors can be much more stable than their n-counterparts with respect to anodic dissolution. The long-term stability of the p-type GaAs-based PEC cell in I^-/I_3^- or other redox couples is under investigation. Although the p-type GaAs-based cells show low open-circuit photovoltages, we are encouraged by the fact that their quantum yields for electron flow can approach 100%, if a suitable redox couple is used.

A final aspect worth discussing is the lack of hydrogen evolution on p-GaAs even under conditions where photogeneration of reduced forms at more negative potentials (e.g. Eu(II)) occurs. This suggests that

large overpotentials exist for hydrogen evolution at the electrode surface and, as for metal electrodes in ordinary electrochemical experiments, catalytic surfaces (e.g. containing Pt or other transition metal) will be required for efficient hydrogen generating p-type materials.

Acknowledgment

The support of this research by the Office of Naval Research is gratefully acknowledged.

TABLE I: Voltammetric Data and Onset Potential of Photocurrent[a]

Redox couple	V°, V vs. SCE[c]	V_{on}, V vs. SCE	$\Delta V = V_{on} - V^\circ$, V
I^-/I_3^- (1 M H^+)	0.29	0.75	0.46
Fe^{2+}/Fe^{3+} (1 M H_3PO_4)	0.20	0.53	0.33
Sn^{2+}/Sn^{4+} (1 M H^+ and 6 M Br^-)	-0.10	0.30	0.40
Fe(II)-EDTA/Fe(III)-EDTA (pH $\cong$ 5)	-0.15	0.25	0.40
HV^+/HV^{2+} b	-0.45	0.00	0.45
Eu^{2+}/Eu^{3+} (1 M $HClO_4$)	-0.67	-0.17	0.50

a) The onset potential of photocurrent V_{on} here is defined as the potential at which 1% of the limiting or maximal photocurrent is observed.

b) HV = heptyl viologen (1,1'-diheptyl-4,4'-bipyridyl)

c) V° = the standard potential.

TABLE II: PEC Cell Parameters and Stability of p-GaAs Photoelectrodes in Various Redox Couples

Redox Couple	V_{oc},V[a]	j_{ss},mA/cm^2[a]	i_{ss},mA[b]	η,%[b]	η',%[c]	[Ga^{3+}],ppm
I^-(0.75 M)/I_3^-(0.25 M)(1 M H^+)	0.20	30	----	----	95[e]	<1
Fe^{2+}(0.5 M)/Fe^{3+}(0.5 M)(1 M H_3PO_4)	0.15	0.6	0.02	3	24	----
Sn^{2+}(0.5 M)/Sn^{3+}(0.5 M)(1 M H^+ and 6 M Br^-)	0.15	5.0	0.13	16	86	----
Fe(II)-EDTA(0.2 M)/Fe(III)-EDTA (0.2 M) (pH $\cong$ 5)	0.12	2.4	0.06	8	8	----
Eu^{2+}(0.2 M)/Eu^{3+}(0.2 M)(1 M $HClO_4$)	0.40[d]	2.8	0.07	9	30	----

a) Irradiation is with the full visible (longer than 590 nm and also IR filtered) output from a 450 W xenon lamp focused onto the photoelectrode.

b) Quantum efficiency, with 1.6 mW He-Ne laser (632.8 nm) as light source. No external power source was applied on the photoelectrode.

(Continued . . .)

TABLE II (continued)

c) Quantum efficiency, with 1.6 mW He-Ne laser (632.8 nm) as the light source. An external power supply was applied to the cell to get a maximum or limiting photocurrent for the specified redox couple.

d) A Hg counter electrode was used instead of platinum to eliminate the Pt-catalyzed hydrogen reduction of protons by Eu^{2+}.

e) After correction for solution absorption.

References

(1) (a) Laser, D. L.; Bard, A. J. J. Electrochem. Soc. 1976, 123, 1027;

(b) Hardee, K. L.; Bard, A. J. J. Electrochem. Soc. 1977, 124, 215; 1975, 122, 122;

(c) Frank, S. N.; Bard, A. J. J. Am. Chem. Soc. 1977, 99, 303, 4667;

(d) Kohl, P. A.; Bard, A. J. J. Electrochem. Soc. 1979, 126, 59;

(e) Kohl, P. A.; Bard, A. J. J. Electrochem. Soc. 1979, 126, 603;

(f) Noufi, R. N.; Kohl, P. A.; Bard, A. J. J. Electrochem. Soc. 1978, 124, 375;

(g) Noufi, R. N.; Kohl, P. A.; Frank, S. N.; Bard, A. J. J. Electrochem. Soc. 1978, 125, 246.

(2) (a) Ellis, A. B.; Kaiser, S. W.; Wrighton, M. S. J. Am. Chem. Soc. 1976, 98, 1635, 6418, 6855;

(b) Ellis, A. B.; Kaiser, S. W.; Bolts, J. M.; Wrighton, M. S. J. Am. Chem. Soc. 1977, 99, 2839, 2848;

(c) Wrighton, M. S.; Ginley, D. S.; Wolczanski, P. T.; Ellis, A. B.; Morse, D. L.; Linz, A. Proc. Nat. Acad. Sci. U.S.A. 1975, 72, 1518;

(d) Wrighton, M. S.; Morse, D. L.; Ellis, A. B.; Ginley, D. S.; Abrahamson, H. B. J. Am. Chem. Soc. 1976, 98, 2774.

(3) (a) Miller, B.; Heller, A. Nature (London) 1976, 262, 680.

(b) Chang, K.-C.; Heller, A.; Schwartz, B.; Menezes, S.; Miller, B. in "Semiconductor Liquid-Junction Solar Cells". A. Heller (Ed.) Proceedings Volume 77-3, The Electrochem. Soc., Inc.: Princeton, N. J., 1977; Page 132.

(4) Tributsch, H. Ber. Bunsenges. Phys. Chem. 1977, 81, 361.

(5) Bolts, J. M.; Ellis, A. B.; Legg, K. D.; Wrighton, M. S. J. Am. Chem. Soc. 1977, 99, 4826.

(6) Gerischer, H.; Mattes, I. Z. Phys. Chem. NF 1966, 49, 112.

(7) Tomkiewicz, M; Woodall, J. M. Science 1977, 196, 990.

(8) Ohashi, K; McCann, J.; Bockris, J. O'M. Nature (London) 1977, 266, 610.

(9) (a) Mead, C. A. Solid-State Electron. 1966, 9, 1023.

(b) Pugh, D. Phys. Rev. Lett. 1964, 12, 390.

(c) Hovel, H. J. Solar Cells, Vol. 11 in the series "Semiconductors and Semimetals, edited by R. K. Willardson and A. C. Beer; Academic: New York, 1975.

(10) Memming, R. in "Semiconductor Liquid-Junction Solar Cells". A. Heller (Ed.) Proceedings of a conference on the Electrochemistry and Physics of Semiconductor Liquid Interfaces under Illumination held at Airlie, Virginia, May 3-5, 1977. The Electrochemical Society: Princeton, N. J., Page 38.

(11) Malpas, R. E.; Itaya, K.; Bard, A. J. J. Am. Chem. Soc. 1979, 101, 2535.

(12) Bard, A.J.; Bocarsly, A.B.; Fan, F-R. F.; Walton, E.G.; Wrighton, M.S. J. Am. Chem. Soc. 1980, 102, 0000 (preceding paper in this issue).

(13) (a) Gerischer, H. Adv. Electrochem. Eng. 1961, 1, 139;

(b) Gerischer, H. in "Physical Chemistry: An Advanced Treatise". Vol. 9A; edited by Eyring, D. Henderson, and W. Jost; Academic Press: New York, 1970.

(14) Kurtin, S.; Mead, C. A. Phys. Rev. Lett. 1969, 22, 1433.

(15) Kohl, P. A.; Bard, A. J. J. Electrochem. Soc. 1979, 126, 598.

(16) Bocarsly, A. B.; Bookbinder, D.C.; Dominey, R.N.; Lewis, N.S.; Wrighton, M.S. J. Am. Chem. Soc. 1980, 102, 0000 (following paper in this issue).

(17) (a) Gerischer, H. J. Electroanal. Chem. 1977, 82, 133.

(b) Bard, A.J.; Wrighton, M.S. J. Electrochem. Soc. 1977, 124, 1706.

(c) Park, S.-M.; Barber, M.E. J. Electroanal. Chem. 1979, 99, 67.

Figure Captions

Figure 1 Voltammetric curves of Pt and p-GaAs electrodes in 1.0 M HI solution.

1. Dark cyclic voltammogram on p-GaAs. Scan rate, 100 mV/sec. Initial potential, s, 0.00 V vs. SCE (with or without added I_2).

2. Current-potential curves under illumination by red light on p-GaAs. Scan rate, 5 mV/sec. Initial potential 0.78 V vs. SCE. Solution contained 0.25 M I_2. The photocurrent was measured by phase-sensitive detection technique. a. Solution was not stirred. b. Solution was stirred.

3. Cyclic voltammetry on Pt. Scan rate, 100 mV/sec. Initial potential 0.28 V vs. SCE. Solution contained 0.25 M I_2.

4. Current-potential curve under illumination with red light on p-GaAs in 1.0 M HI. Scan rate, 5 mV/sec. Initial potential 0.10 V vs. SCE. The photocurrent was measured by phase-sensitive detection technique (without added I_2).

Figure 2 Schematic diagram of the energy levels at the p-GaAs/electrolyte interface. E_c, E_f, and E_v denote the conduction band edge, the Fermi energy, and the valence band edge of p-GaAs, respectively.

Figure 3 Voltammetric curves of Pt and p-GaAs electrodes in various solutions. Initial potential 0.00 V vs. SCE.

a. On p-GaAs. 0.1 M KBr (pH $\cong$ 6). Scan rate 100 mV/sec. In the dark.

b. On p-GaAs. 0.1 M KBr (pH $\cong$ 6). Scan rate 100 mV/sec. In the light.

c-1. On p-GaAs under illumination. 0.1 M KBr and 2×10^{-2} M heptyl-viologen^{2+} (pH $\cong$ 6). Scan rate 100 mV/sec.

c-2. On p-GaAs in the dark right after c-1. 0.1 M KBr and $2x10^{-2}$ M heptyl-viologen^{2+} (pH ≅ 6). Scan rate 100 mV/sec.

d. On Pt. 0.1 M KBr and $2x10^{-2}$ M heptyl-viologen^{2+} (pH ≅ 6). Scan rate 100 mV/sec.

e. Current-potential curve under illumination with red light on p-GaAs in 1.0 M $HClO_4$ containing 0.20 M Eu^{2+} (pH ≅ 0). Scan rate 5 mV/sec. The photocurrent was measured by phase-sensitive detection technique.

f. Current-potential curve under illumination with red light on p-GaAs in 1.0 M $HClO_4$. The photocurrent was measured by phase-sensitive detection technique.

Figure 4 Current-potential curves for p-GaAs and Pt electrodes in various electrolyte solutions.

(a) 0.20 M Fe(III)-EDTA and 0.20 M Fe(II)-EDTA (pH ≅ 5).

1. On Pt. Scan rate 100 mV/sec.
2. On p-GaAs under chopped red light. Scan rate 10 mV/sec.
3. On p-GaAs in the dark. Scan rate 100 mV/sec.

(b) 1.0 M H_3PO_4 containing 0.5 M Fe(II) and 0.5 M Fe(III).

4. On Pt. Scan rate 100 mV/sec.
5. On P-GaAs under chopped red light. Scan rate 10 mV/sec.
6. On p-GaAs in the dark. Scan rate 100 mV/sec.

(c) 1 M H^+, 0.5 M Sn(II), 0.5 M Sn(IV), and 6.0 M Br^-.

7. On Pt. Scan rate 100 mV/sec.
8. On p-GaAs under chopped red light. Scan rate 10 mV/sec.
9. On p-GaAs in the dark. Scan rate 100 mV/sec.

Figure 5 Schematic representation of a regenerative semiconductor/liquid junction photovoltaic cell containing a redox couple R/O.

Figure 6 Quantum efficiency vs. wavelength for a p-GaAs/I^- (0.75 M), I_3^- (0.25 M), H^+ (1.0 M)/Pt PEC cell. Monochromatic light intensity 5-8 mW/cm^2.

Triangles: corrected for solution absorption.

Circles: without correcting for solution absorption.

Figure 7 Steady state current density - voltage relation for a p-GaAs/I^- (0.75 M), I_3^- (0.25 M), H^+ (1.0 M)/Pt PEC cell. Irradiation was with the full visible (longer than 590 nm and also IR filtered) output from a 450 W xenon lamp focused onto the photoelectrode. The optical path through the solution was about 1 cm.

Figure 8 Time dependence of the photocurrent of a p-GaAs/I^- (0.75 M), I_3^- (0.25 M), H^+ (1.0 M)/Pt PEC cell. The cell was run at maximum power by connecting through a load resistance of 150 Ω. The solution was not stirred. Irradiation was with the red light (590 nm cut-on and also IR filtered) from a 450 W Xe-lamp focused onto the photoelectrode. The optical path through the solution was about 1 cm.

Figure 9 Schematic representation of the surface barrier at a semiconductor/solution interface. E_c = conduction band edge; E_f = Fermi level; E_v = valence band edge of a semiconductor; V° = standard potential of a redox couple; V_{fb} = flat-band potential of a semiconductor electrode; j = current density.

a. Ideal model.

Voc = Open-circuit photovoltage of a PEC cell.

b. Recombinative model (Curves 1 and 2 for n-SC, 3 and 4 for p-SC). s.s. = surface states or recombination centers; 1 and 3 = current-potential curves under illumination without recombination; 2 and 4 = current-potential curves under illumination with recombination; Voc = open-circuit photovoltage.

Figure 9 (continued)

c. Surface layer controlled model (Curves 1 -4 for n-SC and 5-8 for p-SC). 1 and 5 = current-potential curves in the dark without recombination; 3 and 8 = current-potential curves under illumiantion without recombination; 2 and 6 = current-potential curves in the dark with recombination; 4 and 7 = current-potential curves under illumination with recombination; E_s = surface state energies; V_s = potential corresponding to E_s; Voc' = open-circuit photovoltage with recombination; Voc = open-circuit photovoltage without recombination.

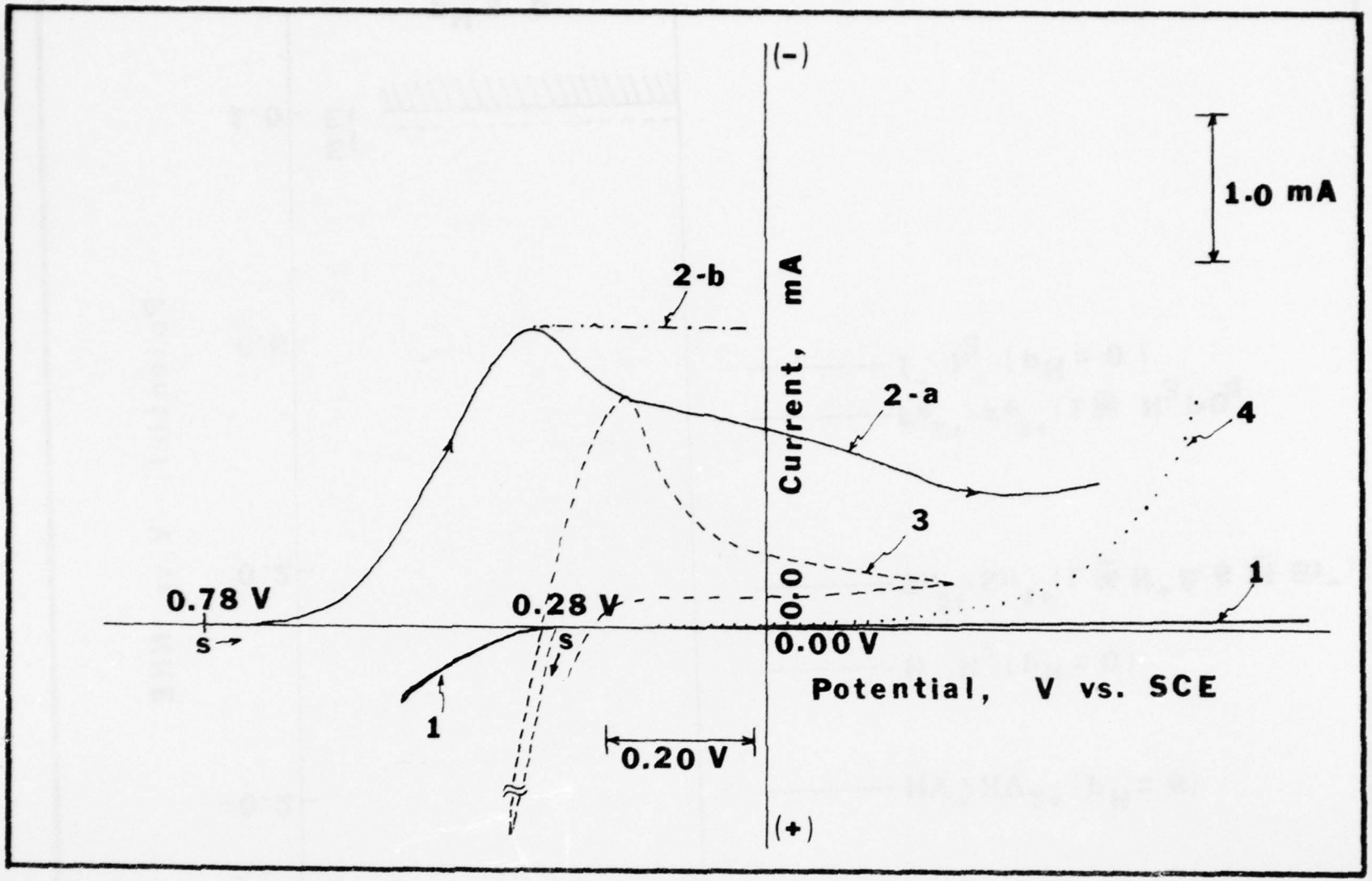
(-)
1.0 mA
2-b
Current, mA
2-a
4
3
1
0.78 V
0.28 V
0.0
0.00 V
s
s
Potential, V vs. SCE
1
0.20 V
(+)

Fig 1

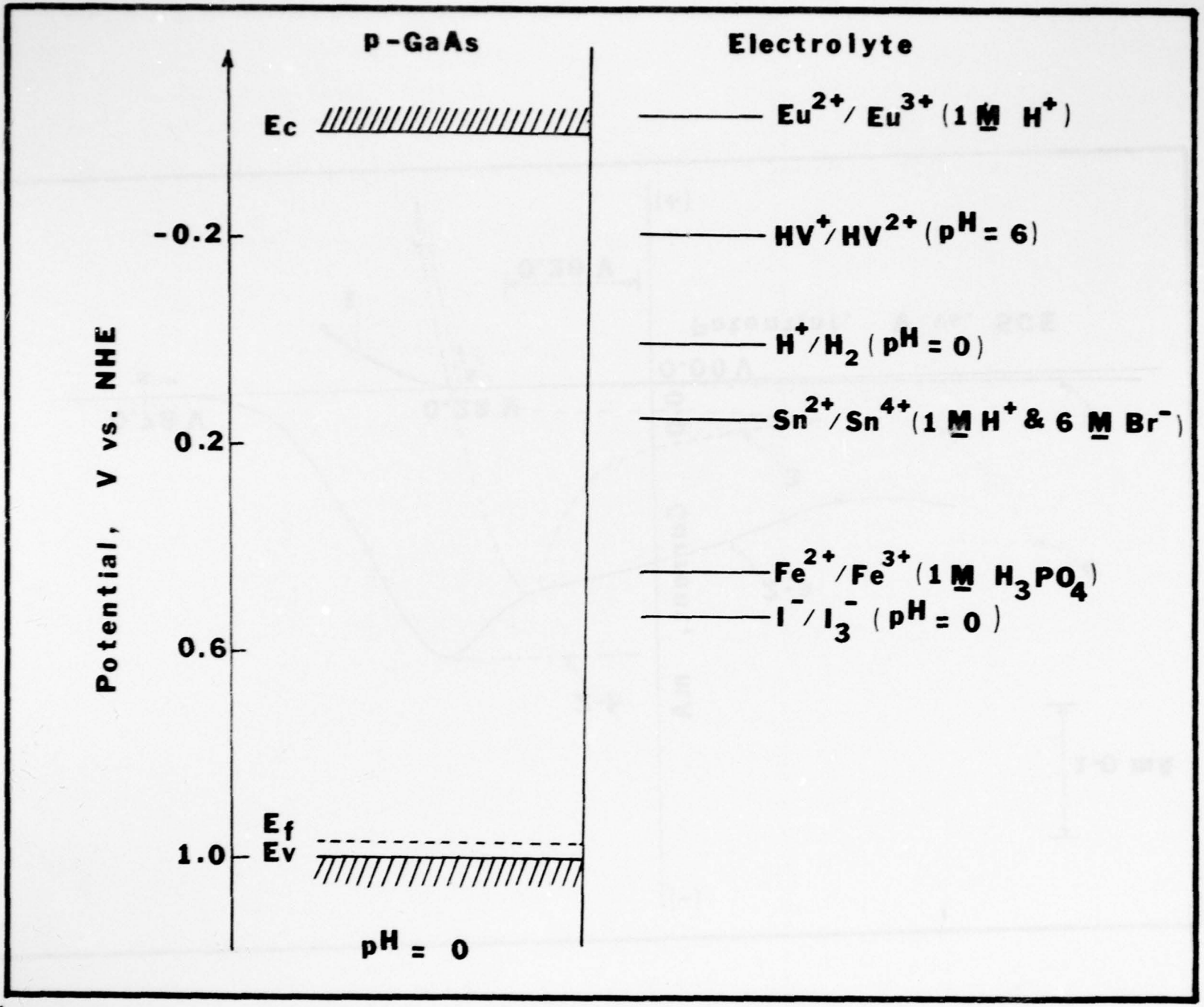
p-GaAs
Electrolyte
Ec
Ef
Ev
-0.2
0.2
0.6
1.0
Potential, V vs. NHE
pH = 0
Eu2+/ Eu3+ (1 M H+)
HV+/HV2+ (pH = 6)
H+/H2 (pH = 0)
Sn2+/Sn4+ (1 M H+ & 6 M Br-)
Fe2+/Fe3+ (1 M H3PO4)
I-/I3- (pH = 0)

Fig 2

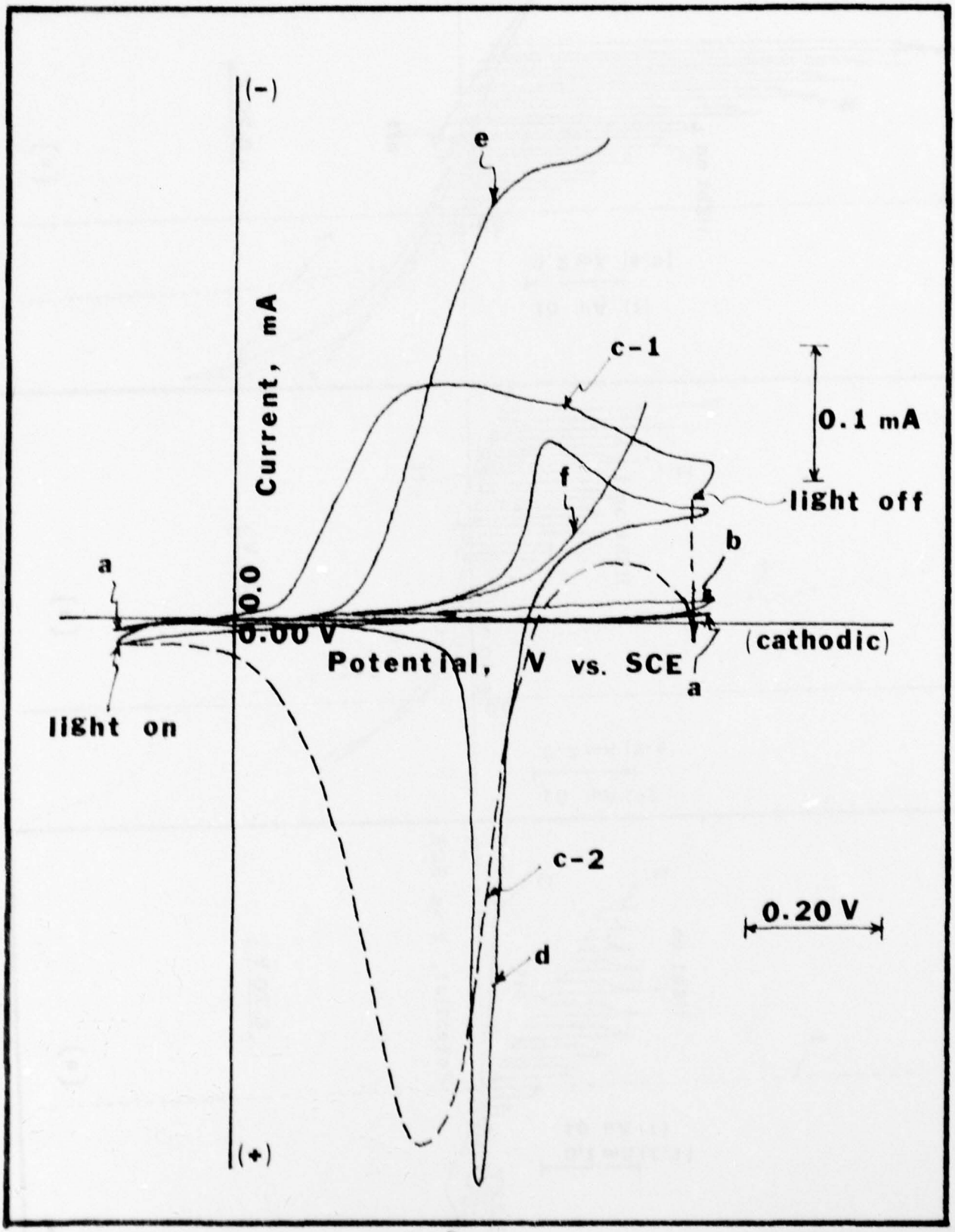
(-)
Current, mA
(+)
e
c-1
0.1 mA
light off
f
b
a
0.0
0.00 V
Potential, V vs. SCE
(cathodic)
a
light on
c-2
0.20 V
d

Fig 3

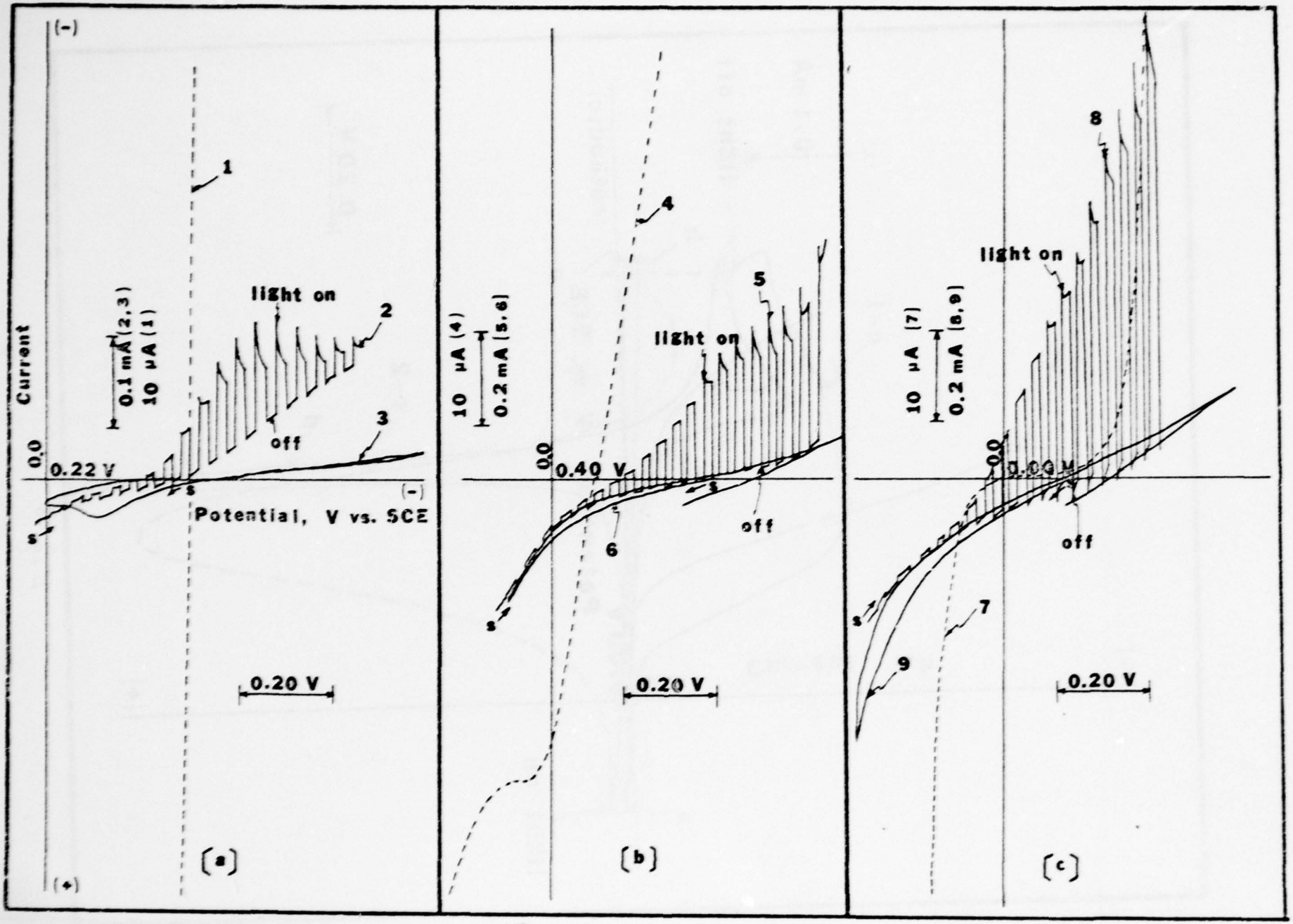
(-)
Current
(+)
0.1 mA (2,3)
10 μA (1)
light on
off
0.0
0.22 V
(-)
Potential, V vs. SCE
0.20 V
(a)
10 μA (4)
0.2 mA (5,6)
light on
off
0.0
0.40 V
0.20 V
(b)
10 μA (7)
0.2 mA (8,9)
light on
off
0.0
0.20 V
(c)

Fig 4

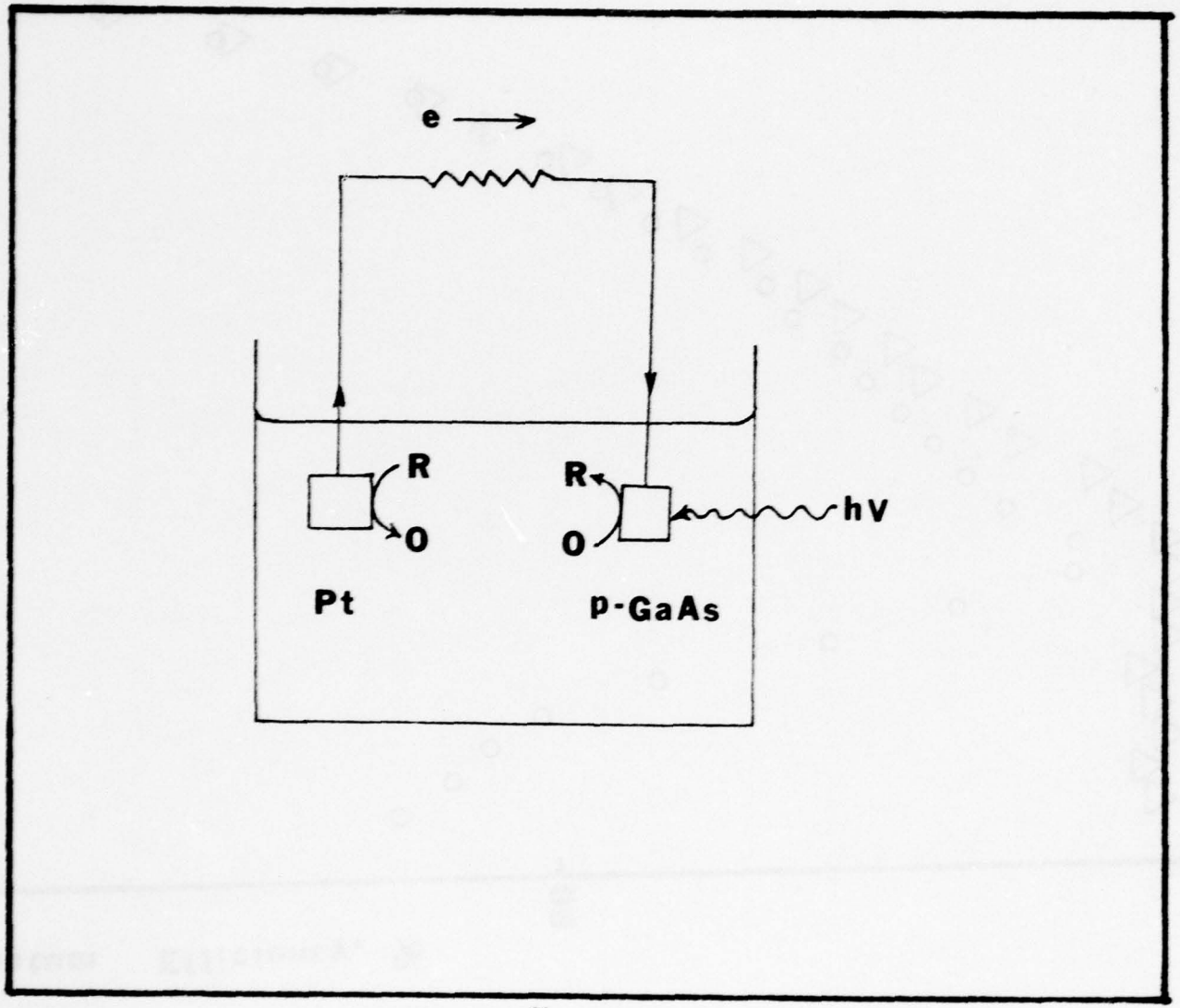

Fig 5

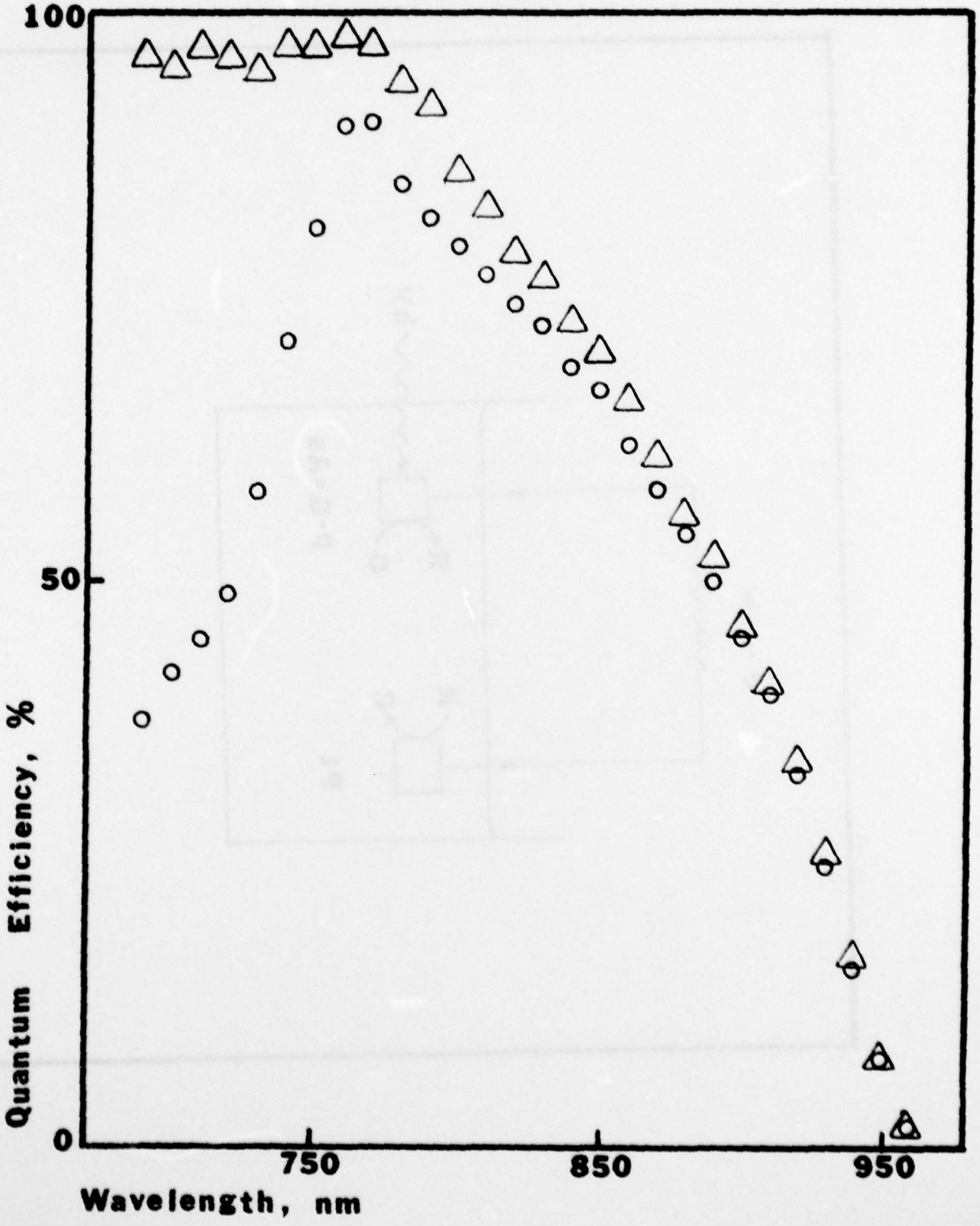

Fig 6

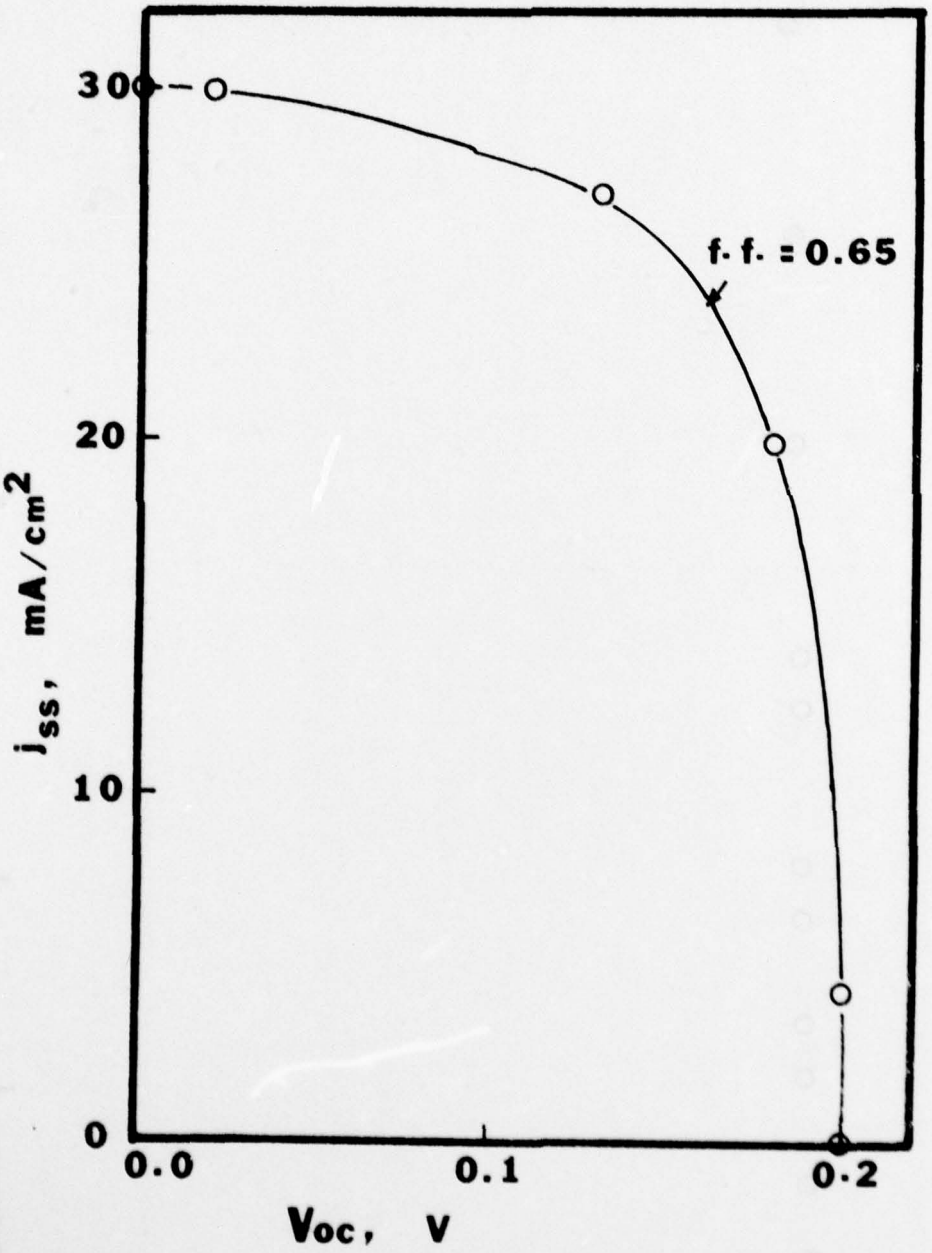

Fig 7

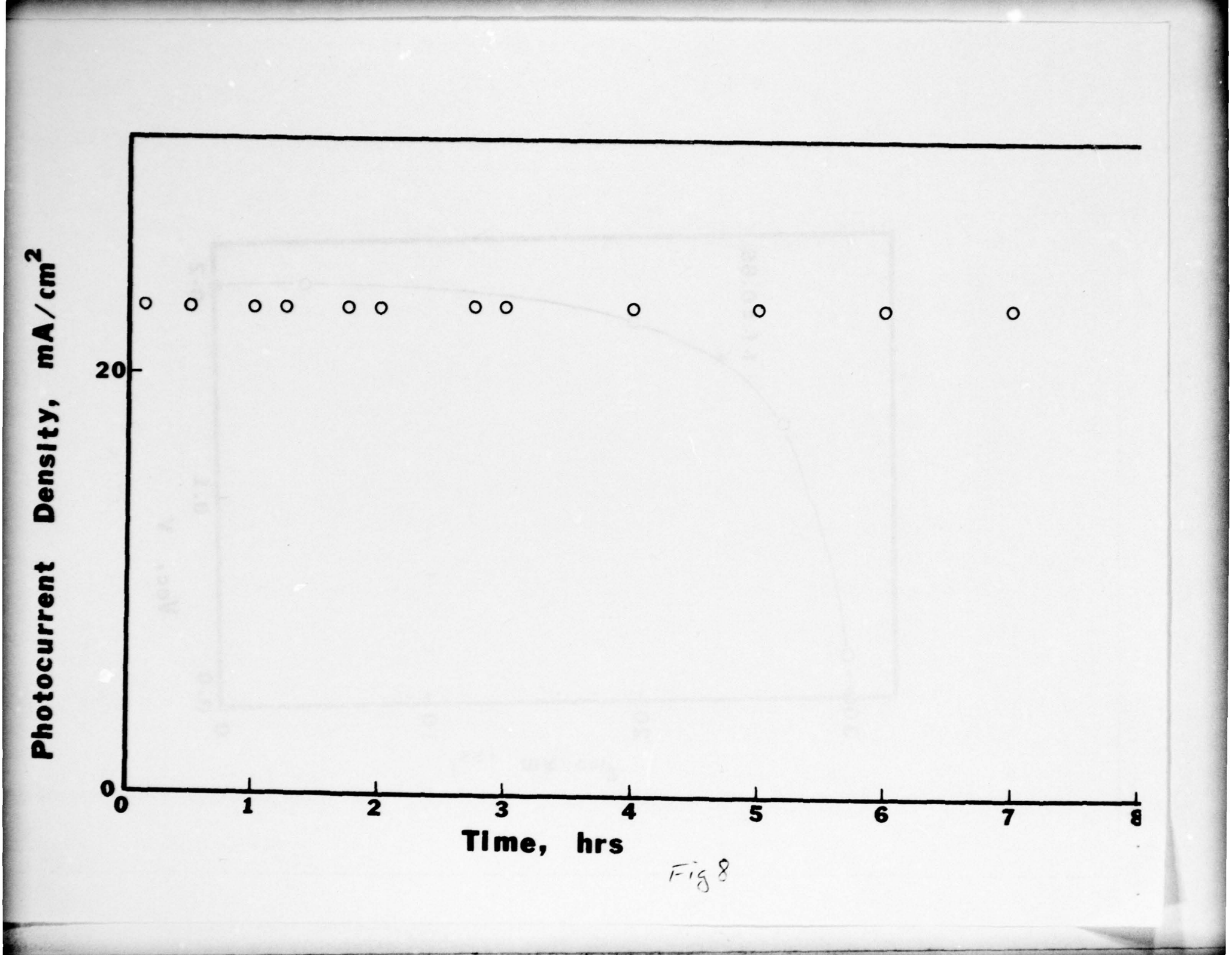

Fig 8

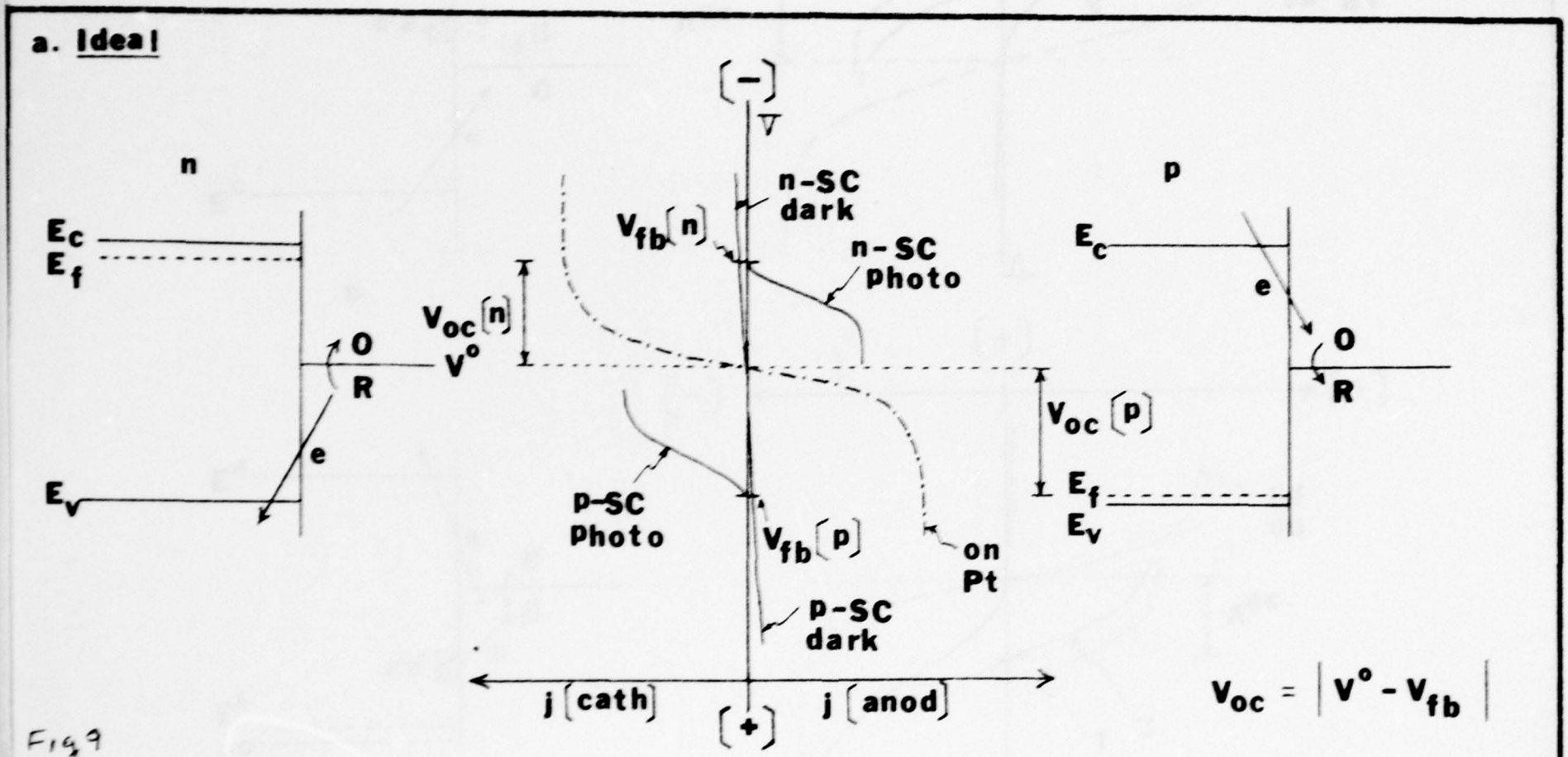
a. Ideal
n
p
(−)
V
n-SC dark
n-SC photo
V_{fb} (n)
V_{oc} (n)
E_c
E_f
E_v
O
R
V^o
e
p-SC Photo
V_{fb} (p)
p-SC dark
on Pt
V_{oc} (p)
j (cath)
j (anod)
(+)
$V_{oc} = |V^o - V_{fb}|$

Fig 9

b. Recombinative

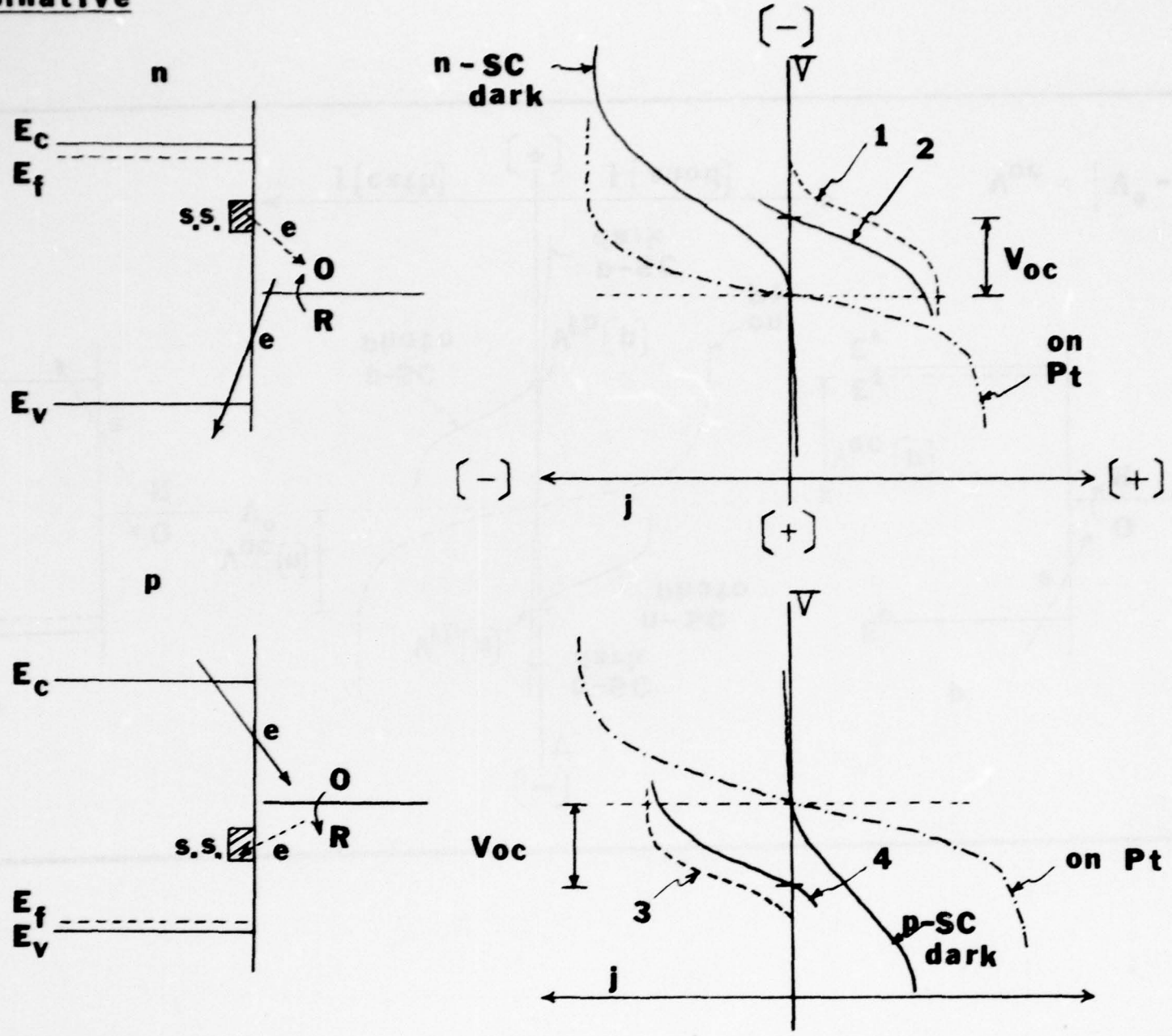

Fig 9

c. Surface Layer Controlled

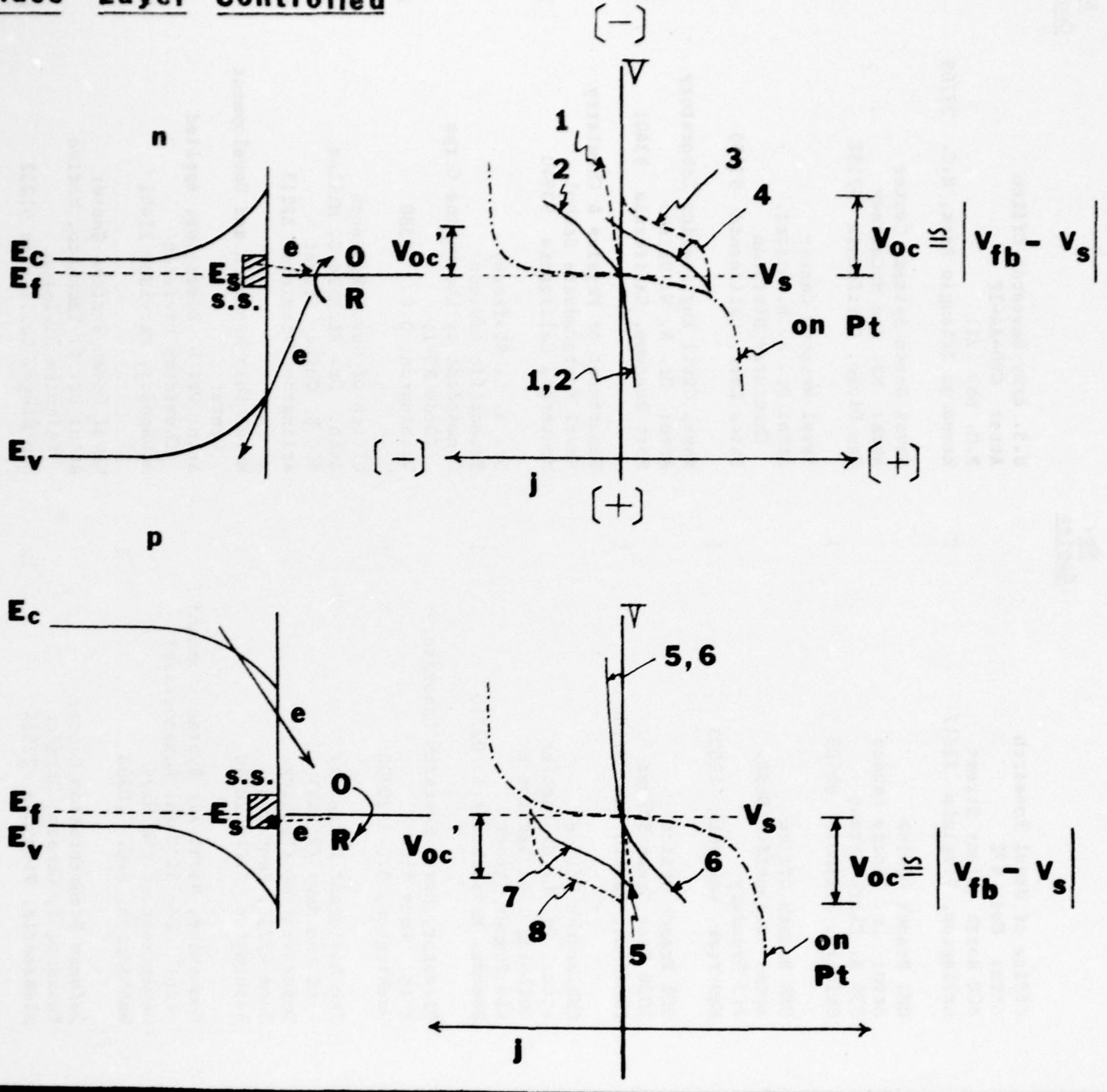

Fig 9

P4-2/A23

472:GAN:716:tam
78u472-608

TECHNICAL REPORT DISTRIBUTION LIST, GEN

	No. Copies
Office of Naval Research Attn: Code 472 800 North Quincy Street Arlington, Virginia 22217	2
ONR Branch Office Attn: Dr. George Sandoz 536 S. Clark Street Chicago, Illinois 60605	1
ONR Branch Office Attn: Scientific Dept. 715 Broadway New York, New York 10003	1
ONR Branch Office 1030 East Green Street Pasadena, California 91106	1
ONR Branch Office Attn: Dr. L. H. Peebles Building 114, Section D 666 Summer Street Boston, Massachusetts 02210	1
Director, Naval Research Laboratory Attn: Code 6100 Washington, D.C. 20390	1
The Assistant Secretary of the Navy (R,E&S) Department of the Navy Room 4E736, Pentagon Washington, D.C. 20350	1
Commander, Naval Air Systems Command Attn: Code 310C (H. Rosenwasser) Department of the Navy Washington, D.C. 20360	1
Defense Documentation Center Building 5, Cameron Station Alexandria, Virginia 22314	12
Dr. Fred Saalfeld Chemistry Division Naval Research Laboratory Washington, D.C. 20375	1
U.S. Army Research Office Attn: CRD-AA-IP P.O. Box 1211 Research Triangle Park, N.C. 27709	1
Naval Ocean Systems Center Attn: Mr. Joe McCartney San Diego, California 92152	1
Naval Weapons Center Attn: Dr. A. B. Amster, Chemistry Division China Lake, California 93555	1
Naval Civil Engineering Laboratory Attn: Dr. R. W. Drisko Port Hueneme, California 93401	1
Department of Physics & Chemistry Naval Postgraduate School Monterey, California 93940	1
Dr. A. L. Slafkosky Scientific Advisor Commandant of the Marine Corps (Code RD-1) Washington, D.C. 20380	1
Office of Naval Research Attn: Dr. Richard S. Miller 800 N. Quincy Street Arlington, Virginia 22217	1
Naval Ship Research and Development Center Attn: Dr. G. Bosmajian, Applied Chemistry Division Annapolis, Maryland 21401	1
Naval Ocean Systems Center Attn: Dr. S. Yamamoto, Marine Sciences Division San Diego, California 91232	1
Mr. John Boyle Materials Branch Naval Ship Engineering Center Philadelphia, Pennsylvania 19112	1

P4-2/A25

472:GAN:716:tam
78u472-608

TECHNICAL REPORT DISTRIBUTION LIST, GEN

	No. Copies
Dr. Rudolph J. Marcus Office of Naval Research Scientific Liaison Group American Embassy APO San Francisco 96503	1
Mr. James Kelley DTNSRDC Code 2803 Annapolis, Maryland 21402	1

TECHNICAL REPORT DISTRIBUTION LIST, 359

	No. Copies
Dr. Paul Delahay Department of Chemistry New York University New York, New York 10003	1
Dr. E. Yeager Department of Chemistry Case Western Reserve University Cleveland, Ohio 41106	1
Dr. D. N. Bennion Chemical Engineering Department University of California Los Angeles, California 90024	1
Dr. R. A. Marcus Department of Chemistry California Institute of Technology Pasadena, California 91125	1
Dr. J. J. Auborn Bell Laboratories Murray Hill, New Jersey 07974	1
Dr. Adam Heller Bell Laboratories Murray Hill, New Jersey 07974	1
Dr. T. Katan Lockheed Missiles & Space Co, Inc. P.O. Box 504 Sunnyvale, California 94088	1
Dr. Joseph Singer, Code 302-1 NASA-Lewis 21000 Brookpark Road Cleveland, Ohio 44135	1
Dr. B. Brummer EIC Incorporated 55 Chapel Street Newton, Massachusetts 02158	1
Library P. R. Mallory and Company, Inc. Northwest Industrial Park Burlington, Massachusetts 01803	1
Dr. P. J. Hendra Department of Chemistry University of Southhampton Southhampton SO9 5NH United Kingdom	1
Dr. Sam Perone Department of Chemistry Purdue University West Lafayette, Indiana 47907	1
Dr. Royce W. Murray Department of Chemistry University of North Carolina Chapel Hill, North Carolina 27514	1
Naval Ocean Systems Center Attn: Technical Library San Diego, California 92152	1
Dr. C. E. Mueller The Electrochemistry Branch Materials Division, Research & Technology Department Naval Surface Weapons Center White Oak Laboratory Silver Spring, Maryland 20910	1
Dr. G. Goodman Globe-Union Incorporated 5757 North Green Bay Avenue Milwaukee, Wisconsin 53201	1
Dr. J. Boechler Electrochimica Corporation Attention: Technical Library 2485 Charleston Road Mountain View, California 94040	1
Dr. P. P. Schmidt Department of Chemistry Oakland University Rochester, Michigan 48063	1
Dr. H. Richtol Chemistry Department Rensselaer Polytechnic Institute Troy, New York 12181	1

TECHNICAL REPORT DISTRIBUTION LIST, 359

	No. Copies
Dr. A. B. Ellis Chemistry Department University of Wisconsin Madison, Wisconsin 53706	1
Dr. M. Wrighton Chemistry Department Massachusetts Institute of Technology Cambridge, Massachusetts 02139	1
Larry E. Plew Naval Weapons Support Center Code 30736, Building 2906 Crane, Indiana 47522	1
S. Ruby DOE (STOR) 600 E Street Washington, D.C. 20545	1
Dr. Aaron Wold Brown University Department of Chemistry Providence, Rhode Island 02192	1
Dr. R. C. Chudacek McGraw-Edison Company Edison Battery Division Post Office Box 28 Bloomfield, New Jersey 07003	1
Dr. A. J. Bard University of Texas Department of Chemistry Austin, Texas 78712	1
Dr. M. M. Nicholson Electronics Research Center Rockwell International 3370 Miraloma Avenue Anaheim, California	1
Dr. Donald W. Ernst Naval Surface Weapons Center Code R-33 White Oak Laboratory Silver Spring, Maryland 20910	1
Dr. R. P. Van Duyne Department of Chemistry Northwestern University Evanston, Illinois 60201	1
Dr. B. Stanley Pons Department of Chemistry Oakland University Rochester, Michigan 48063	1
Dr. Michael J. Weaver Department of Chemistry Michigan State University East Lansing, Michigan 48824	1
Dr. R. David Rauh EIC Corporation 55 Chapel Street Newton, Massachusetts 02158	1
Dr. J. David Margerum Research Laboratories Division Hughes Aircraft Company 3011 Malibu Canyon Road Malibu, California 90265	1
Dr. Martin Fleischmann Department of Chemistry University of Southampton Southampton 509 5NH England	1
Dr. Janet Osteryoung Department of Chemistry State University of New York at Buffalo Buffalo, New York 14214	1
Dr. R. A. Osteryoung Department of Chemistry State University of New York at Buffalo Buffalo, New York 14214	1
Mr. James R. Moden Naval Underwater Systems Center Code 3632 Newport, Rhode Island 02840	1

TECHNICAL REPORT DISTRIBUTION LIST, 359

No.
Copies

Dr. R. Nowak
Naval Research Laboratory
Code 6130
Washington, D.C. 20375

Dr. John F. Houlihan
Shenango Valley Campus
Penn. State University
Sharon, PA 16146